Electronic Supplementary Material (ESI) for Journal of Materials Chemistry A.
This journal is © The Royal Society of Chemistry 2023

# Supplementary Information

## New superionic halide solid electrolytes enabled by aliovalent substitution in $Li_{3-x}Y_{1-x}Hf_xCl_6$ for all-solid-state lithium metal based batteries

Kaiyong Tuo[a], Chunwen Sun[a,*], C.A. López[b,c], Maria Teresa Fernández-Díaz[d], José Antonio Alonso[b]

[a] School of Chemical & Environmental Engineering, China University of Mining and Technology-Beijing, Beijing 100083, P. R. China.

[b] Instituto de Ciencia de los Materiales de Madrid, CSIC, E-28049, Cantoblanco-Madrid, Spain.

[c] INTEQUI (UNSL, CONICET) and Facultad de Química, Bioquímica y Farmacia, UNSL, Chacabuco y Pedernera, San Luis, 5700, Argentina.

[d] Institut Laue Langevin, BP 156X Grenoble, F-38042, France

*Corresponding E-mail address: csun@cumtb.edu.cn (C. Sun)

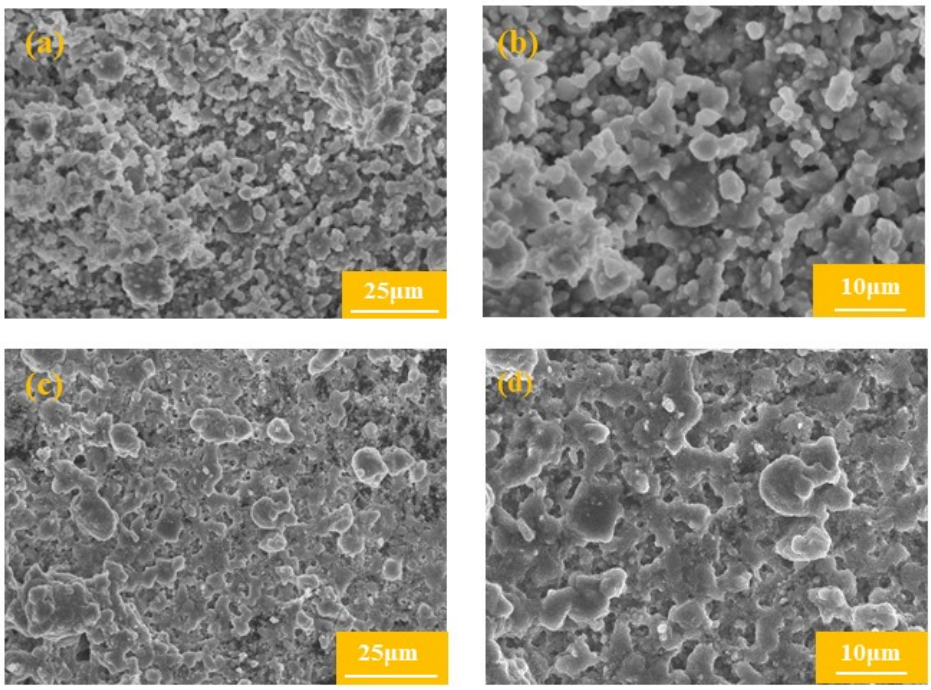


**Figure S1.** SEM images of halide LYC (a、b) and LYHC (c、d) derived from mechanochemical synthesis.

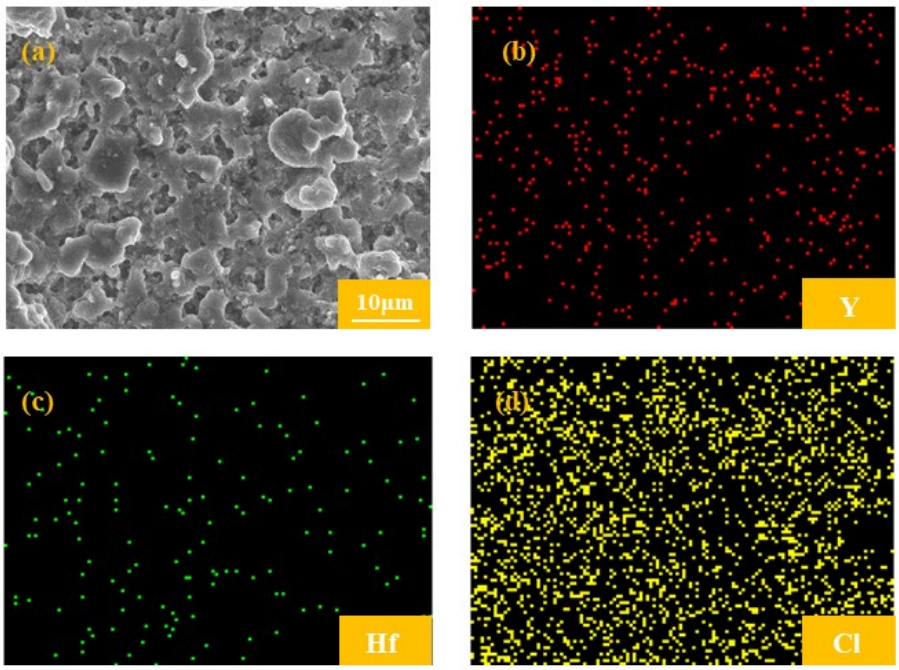


**Figure S2.** The EDS mapping of Y, Hf, and Cl elements for halide LYHC derived from mechanochemical synthesis.

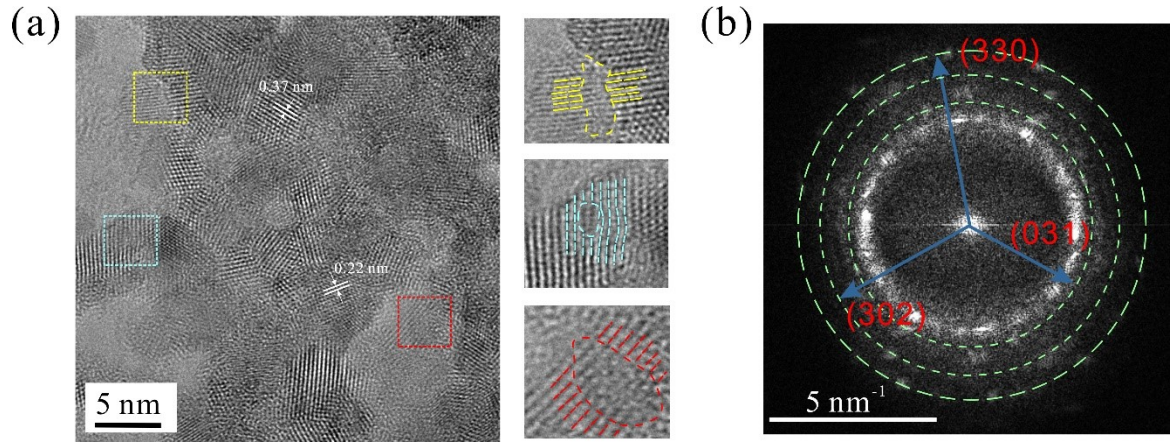


**Figure S3.** HRTEM images (a) and the FFT diffraction pattern (b) of the LYHC halide electrolytes derived from the mechanochemical syntheses.

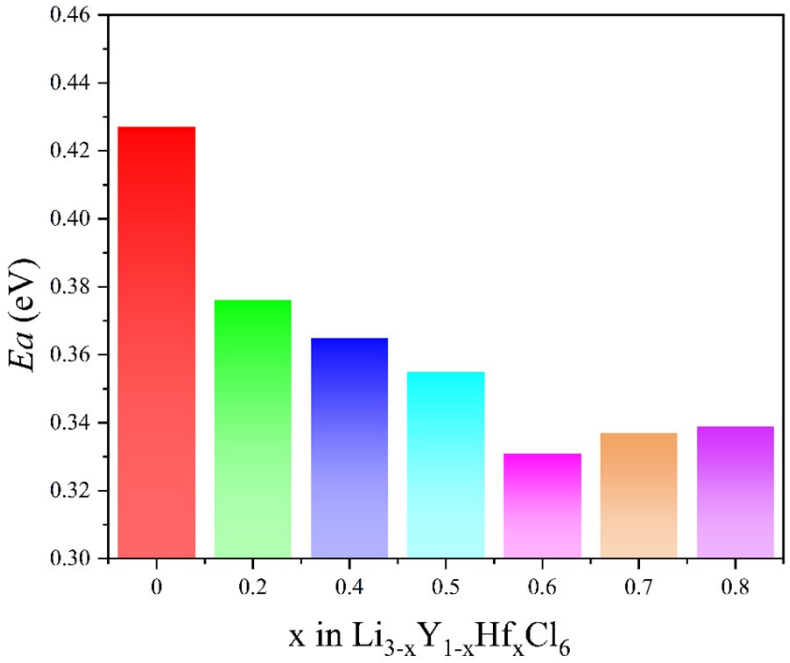


**Figure S4.** The activation energy for $Hf^{4+}$-substituted LYC as a function of x in $Li_{3-x}Y_{1-x}Hf_xCl_6$ ($0 \leqslant x < 1$).

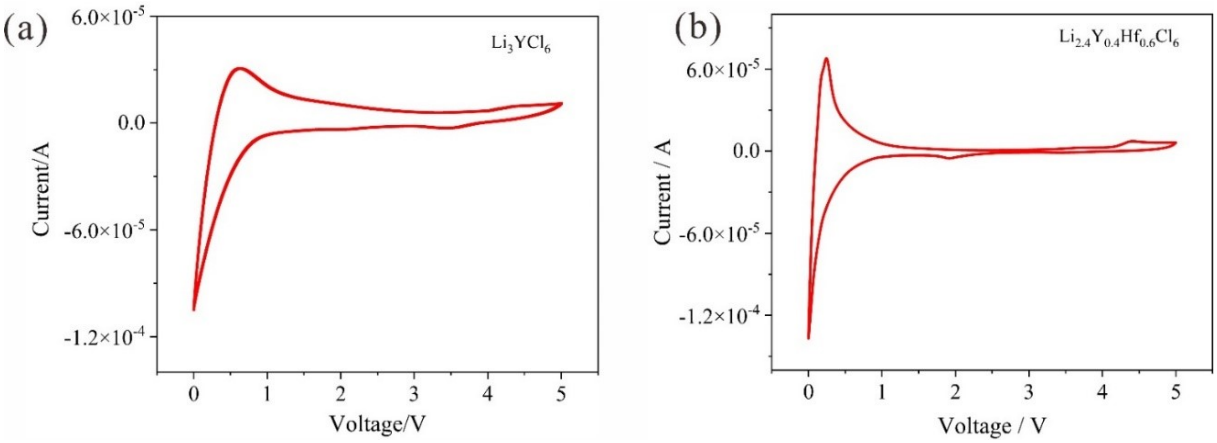


**Figure S5.** Cyclic voltammogram curves of LYC and LYHC performed on the Li/LPSC/halide SSE/halide SSE+C cell at 0.5 mV $s^{-1}$ (halide and carbon mass ratio of 7:3).

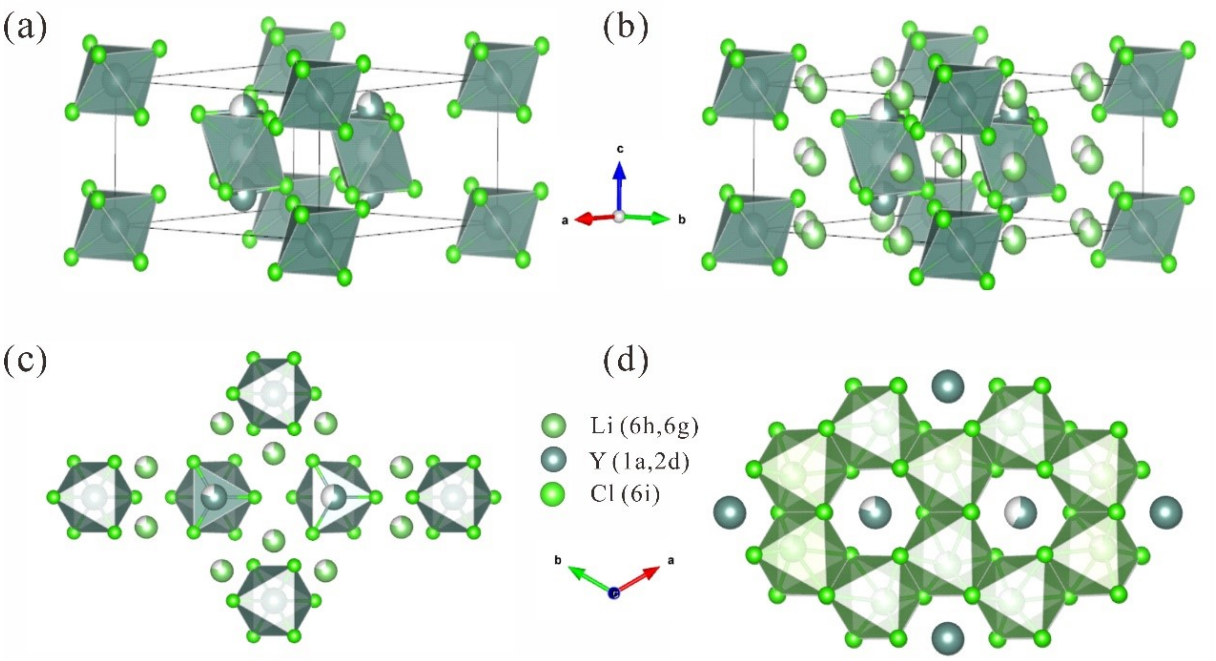


**Figure S6.** Schematic views of the crystal structure of as-milled LYC halide electrolytes, in which Y occupies Wyckoff 1a and 2d position, and Li is found to occupy two different Wyckoff positions, namely, the Wyckoff 6h and 6g position, while the Wyckoff 6i positions are fully occupied by chlorine.

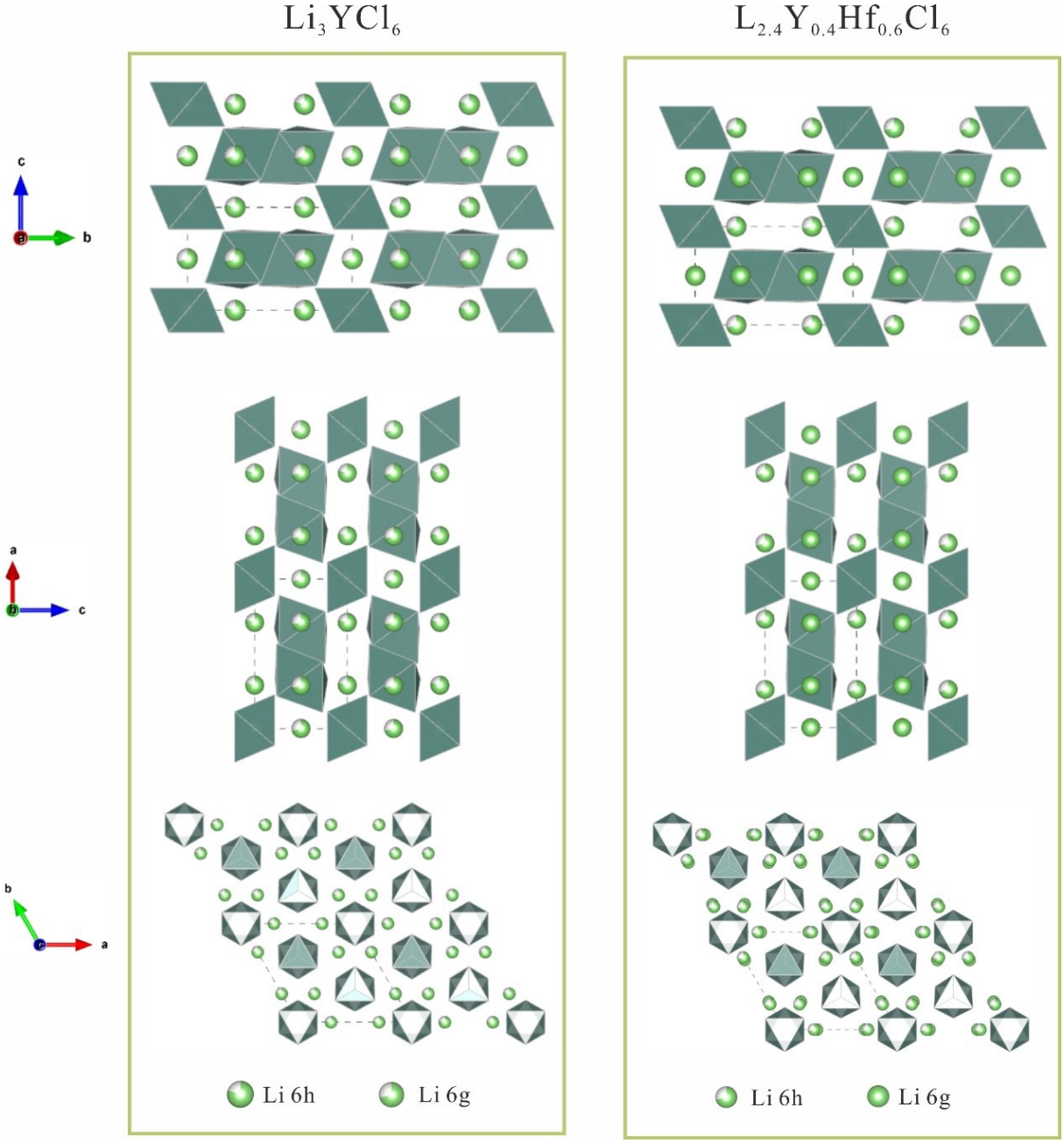


**Figure S7.** The arrangement of three types of lithium ions and the octahedra centred with M ($Y^{3+}$, $Hf^{4+}$) viewed from the [100], [010], and [001] directions in the crystals of (a) LYC and (b) LYHC derived from mechanochemical synthesis.

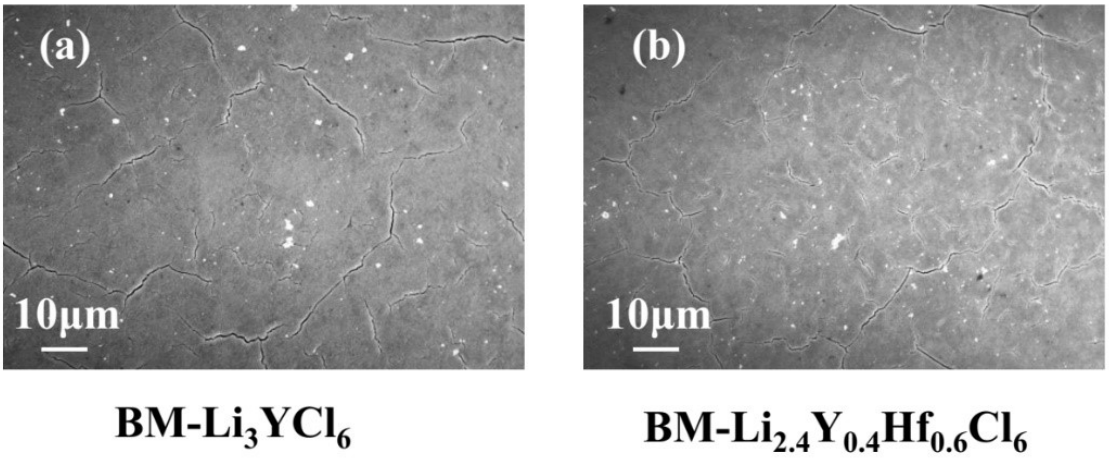


**Figure S8.** SEM images of the surface of BM-LYC and BM-LYHC pellets prepared by cold-pressing at ~3 ton.

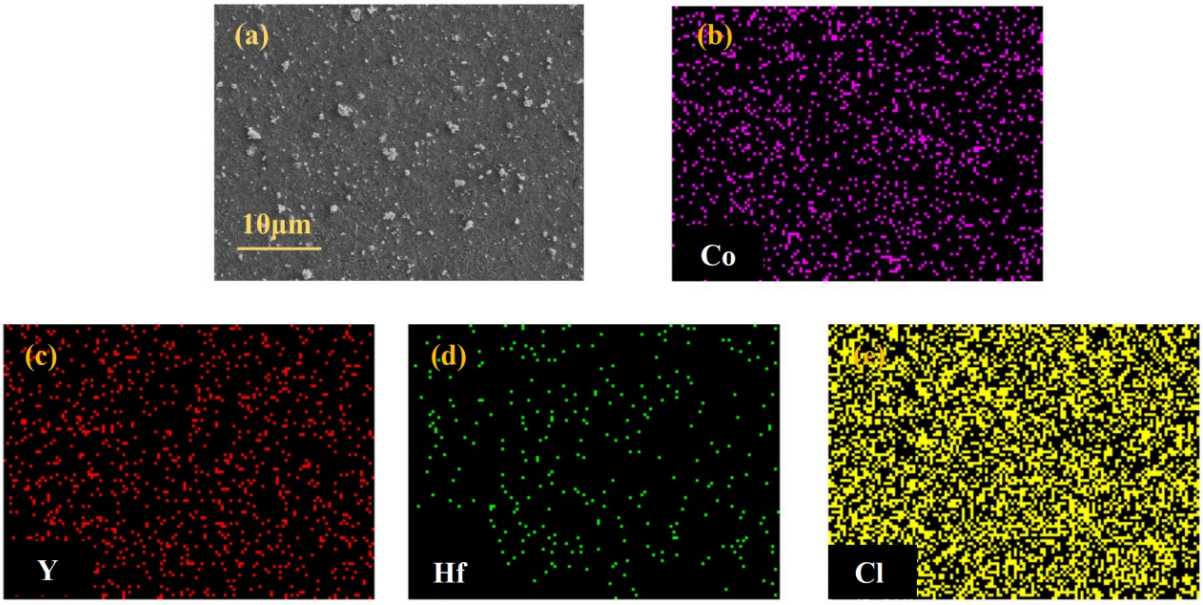


**Figure S9.** SEM images and the corresponding elemental distribution mappings of the $LiCoO_2$ composite cathode pellet in ASSB derived from simple cold-pressing of the as-milled LYHC halide electrolyte.

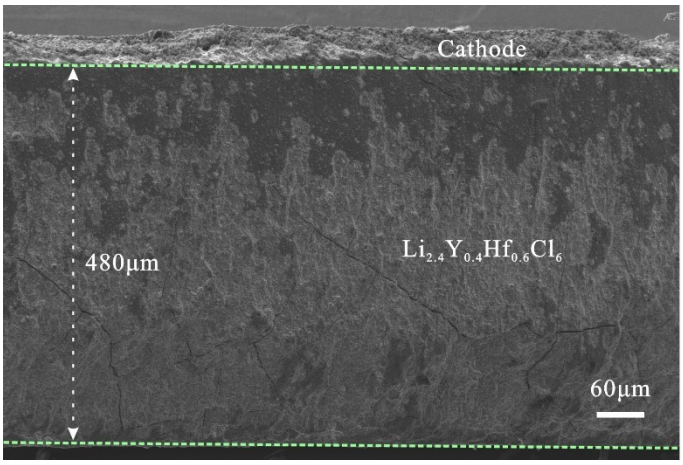


**Figure S10.** Cross-sectional SEM image of the pellet derived from cold-pressing LYHC halide electrolytes and composite cathode.

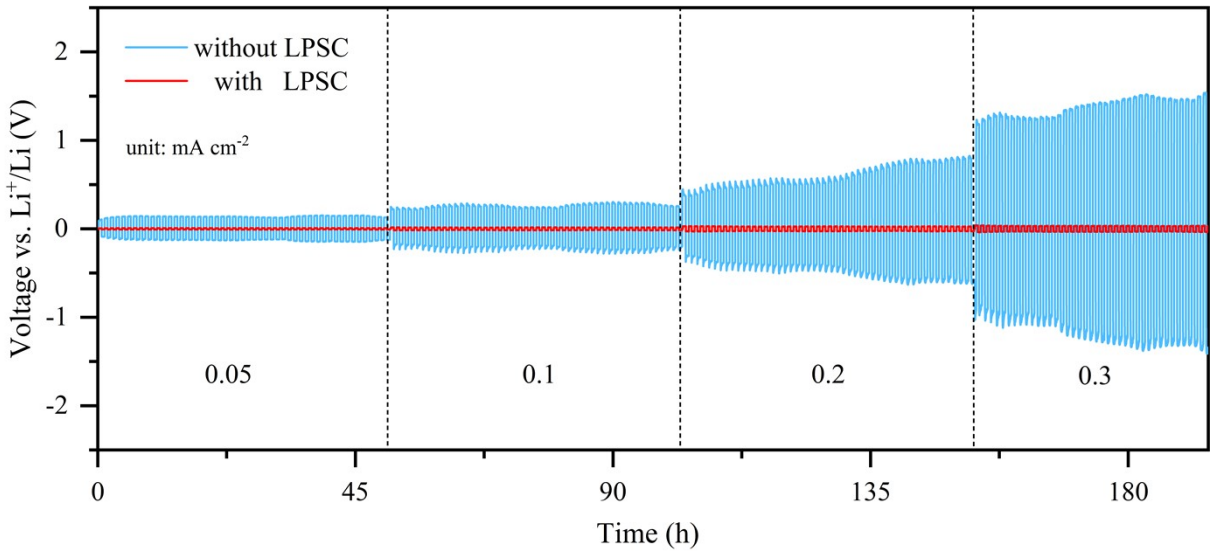


**Figure S11**. Voltage profiles of the Li/LYHC/Li and Li/LPSC/LYHC/LPSC/Li symmetric cell with increased current densities.

The overpotential of symmetric Li/LYHC/Li dramatically increased to about 1500 mV after 180 h cycling. As a sharp contrast, the Li/LPSC/LYHC/LPSC/Li could be stably cycled for up to 180 h with a small overpotential of less than 90 mV, which confirmed that the introduced LPSC layer render the outstanding interfacial stability between anode and halide electrolytes.

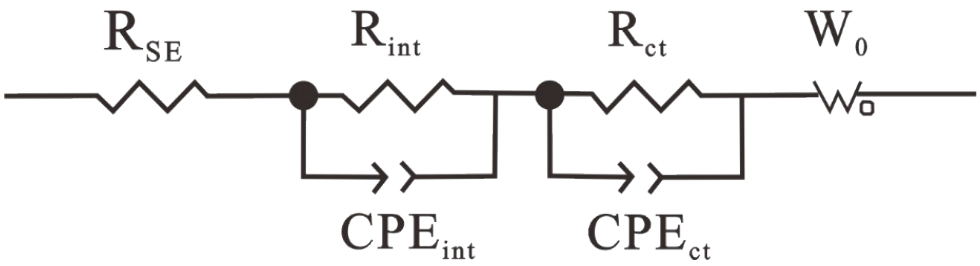


**Figure S12.** The equivalent circuit for fitting the EIS spectra of the ASSBs after 100 cycles.

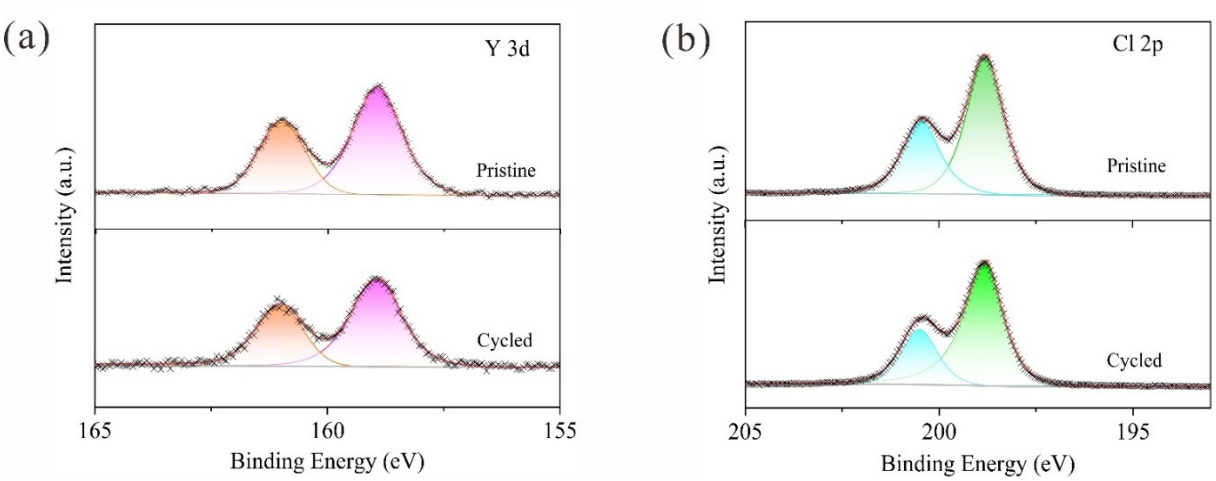


**Figure S13.** XPS spectra of the LYHC composite cathode in ASSBs before cycling and after 100 cycles.

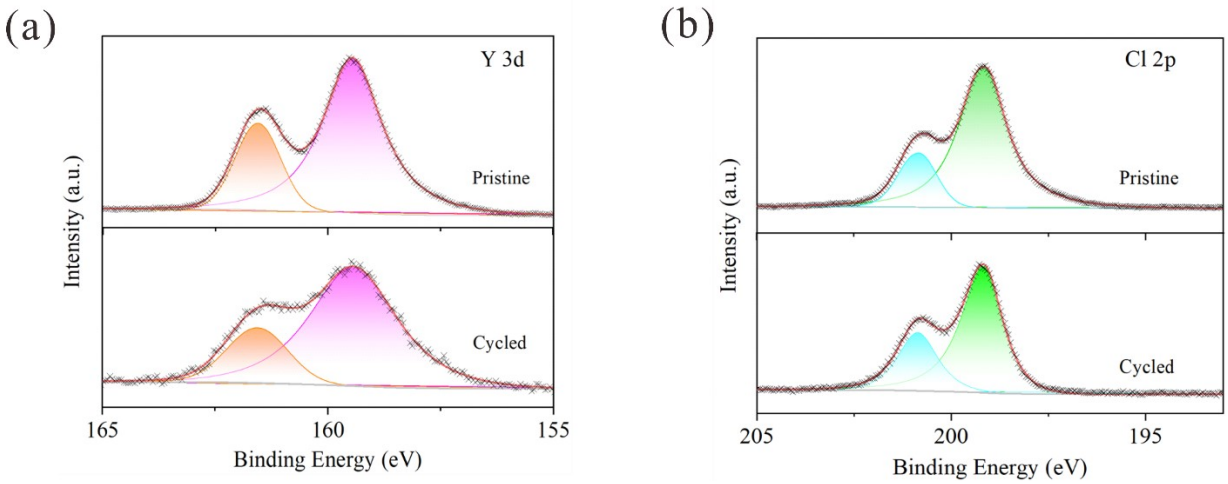


**Figure S14.** XPS spectra of the LYC composite cathode in ASSBs before cycling and after 100 cycles.

**Table S1.** Crystallographic data for mechanochemically synthesized LYC in the trigonal *Pm*1 space group from NPD at 298 K.The refined lattice parameters are a = 11.183(2) Å, c = 6.038(1) Å and V = 654.0(2) Å$^3$.

| Atom | ***Wyckoff Site*** | ***x/a*** | ***y/b*** | ***z/c*** | $B_{iso}$ | $f_{occ}$ |
|---|---|---|---|---|---|---|
| **Li1** | 6*h* | 0.29(2) | 0 | 0.5 | 3.0(1) | 0.7(2) |
| **Li2** | 6*g* | 0.29(2) | 0 | 0 | 3.0(1) | 0.8(2) |
| **Y1** | 1*a* | 0 | 0 | 0 | 3.0(1) | 1 |
| **Y2** | 2*d* | 0.3333 | 0.6666 | 0.79(1) | 2.9(1) | 0.8(1) |
| **Y3** | 2*d* | 0.3333 | 0.6666 | 0.48(8) | 2.9(1) | 0.20(7) |
| **Y4** | 2*d* | 0.3333 | 0.6666 | 0.22(2) | 2.9(1) | 0.6(1) |
| **Cl1** | 6*i* | 0.113(2) | -0.113(2) | 0.785(3) | 0.8(2) | 1 |
| **Cl2** | 6*i* | 0.217(1) | -0.217(1) | 0.237(6) | 0.8(2) | 1 |
| **Cl3** | 6*i* | 0.446(2) | -0.446(2) | 0.735(3) | 0.8(2) | 1 |
| $R_p$ = 2.24%, $R_{wp}$ = 3.06%, $\chi^2$ = 26.0, $R_{Bragg}$ = 9.47% | | | | | | |

**Table S2.** Crystallographic data and Rietveld refinement results for mechanochemically synthesized LYHC in trigonal $P\bar{3}m1$ space group using high-resolution D2B neutron diffractometer at 298 K. The refined lattice parameters are *a* = 11.072(3) Å, *c* = 5.997(4) Å and V = 636.7(5) Å$^3$.

| Atom | ***Wyckoff Site*** | ***x/a*** | ***y/b*** | ***z/c*** | $B_{iso}$ | $f_{occ}$ |
|---|---|---|---|---|---|---|
| **Li1** | 6*h* | 0.286(4) | 0 | 0.5 | 1.0(9) | 1 |
| **Li2** | 6*g* | 0.26(9) | 0 | 0 | 1.0(9) | 0.8 |
| **Y1/Hf1** | 1*a* | 0 | 0 | 0 | 2.8(9) | 1 |
| **Y2/Hf2** | 2*d* | 0.3333 | 0.6666 | 0.8(1) | 1.8(9) | 0.6(2) |
| **Y3/Hf3** | 2*d* | 0.3333 | 0.6666 | 0.5(2) | 1.8(9) | 0.60(6) |
| **Y4/Hf4** | 2*d* | 0.3333 | 0.6666 | 0.2(3) | 1.8(9) | 0.4(1) |
| **Cl1** | 6*i* | 0.115(2) | -0.115(2) | 0.783(3) | 0.8(2) | 1 |
| **Cl2** | 6*i* | 0.217(2) | -0.217(2) | 0.242(6) | 0.8(2) | 1 |
| **Cl3** | 6*i* | 0.442(1) | -0.442(1) | 0.731(4) | 0.8(2) | 1 |
| $R_p$ = 1.98%, $R_{wp}$ = 2.55%, $\chi^2$ = 15.0, $R_{Bragg}$ = 2.26% | | | | | | |

**Table S3.** Percolation Energy and Volume mobility fraction for mechanochemically synthesized LYC and LYHC.

| ion | direction | LYC | LYHC |
|---|---|---|---|
| $Li^+$ | *a*-axis | 2.79 eV | 2.84 eV |
| | *c*-axis | 2.79 eV | 2.84 eV |
| | *Volume mobility* | 7% | 8% |
| $Y^{3+}$ | *a*-axis | 6.82 eV | 4.33 eV |
| | *c*-axis | 2.76 eV | 4.02 eV |
| | *Volume mobility* | 7 % | 5 % |

**Table S4.** Resistance of the ASSBs employed LYHC and LYC after 100 cycles fitted from the equivalent electric circuit.

| | $R_{SE}$ (Ω) | $R_{int}$ (Ω) | $R_{ct}$ (Ω) |
|---|---|---|---|
| **LYHC** | 205.6 | 111.2 | 317.7 |
| **LYC** | 680.1 | 737.3 | 1161.0 |

**Notes and Reference**


1. R. Schlem, A. Banik, S. Ohno, E. Suard and W. G. Zeier, *Chem. Mater.*, 2021, **33**, 327-337.
2. X. Li, M. Liang, J. Sheng, D. Song, H. Zhang, X. Shi and L. Zhang, *Energy Storage Mat.*, 2019, **18**, 100-106.
3. Q. Shao, C. Yan, M. Gao, W. Du, J. Chen, Y. Yang, J. Gan, Z. Wu, W. Sun and Y. Jiang, *ACS Appl. Mater. Interfaces*, 2022, **14**, 8095-8105.